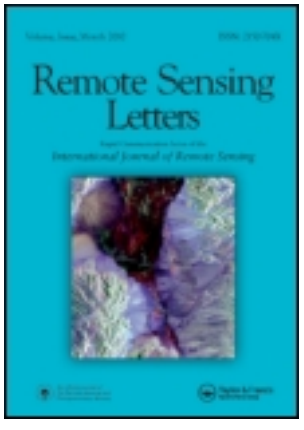

Remote Sensing Letters
Publication details, including instructions for authors and subscription information:
http://www.tandfonline.com/loi/trsl20

Linking ground-based to satellite-derived phenological metrics in support of habitat assessment

Nicholas C. Coops [a], Thomas Hilker [a], Christopher W. Bater [a], Michael A. Wulder [b], Scott E. Nielsen [c], Greg McDermid [d] & Gordon Stenhouse [e]

[a] Faculty of Forest Resources Management, University of British Columbia, Vancouver, BC, Canada

[b] Canadian Forest Service (Pacific Forestry Centre), Natural Resources Canada, Victoria, BC, Canada

[c] Department of Renewable Resources, University of Alberta, Edmonton, AB, Canada

[d] Department of Geography, University of Calgary, Calgary, AB, Canada

[e] Foothills Research Institute, Hinton, AB, Canada

Available online: 04 Aug 2011

To cite this article: Nicholas C. Coops, Thomas Hilker, Christopher W. Bater, Michael A. Wulder, Scott E. Nielsen, Greg McDermid & Gordon Stenhouse (2012): Linking ground-based to satellite-derived phenological metrics in support of habitat assessment, Remote Sensing Letters, 3:3, 191-200

To link to this article: http://dx.doi.org/10.1080/01431161.2010.550330

Remote Sensing Letters
Vol. 3, No. 3, May 2012, 191–200

Linking ground-based to satellite-derived phenological metrics in support of habitat assessment

NICHOLAS C. COOPS*†, THOMAS HILKER†, CHRISTOPHER W. BATER†, MICHAEL A. WULDER‡, SCOTT E. NIELSEN§, GREG MCDERMID¶ and GORDON STENHOUSE|

†Faculty of Forest Resources Management, University of British Columbia, Vancouver, BC, Canada
‡Canadian Forest Service (Pacific Forestry Centre), Natural Resources Canada, Victoria, BC, Canada
§Department of Renewable Resources, University of Alberta, Edmonton, AB, Canada
¶Department of Geography, University of Calgary, Calgary, AB, Canada
|Foothills Research Institute, Hinton, AB, Canada

(*Received 20 October 2010; in final form 19 December 2010*)

Changes in the timing of plant phenology are important indicators of inter-annual climatic variations and are a critical driver of food availability and habitat use for a range of species. A number of remote sensing techniques have recently been developed to observe vegetation cycles throughout the year, including the use of inexpensive visible spectrum digital cameras at the stand level and the use of high temporal frequency Advanced Very High Resolution Radiometer National Oceanic and Atmospheric Administration (AVHRR NOAA) and MODerate resolution Imaging Spectroradiometer (MODIS) imagery at a satellite scale. A fundamental challenge with using satellite data to track plant phenology, however, is the trade-off between the level of spatial detail and the revisit time provided by the sensor, and the ability to verify the interpretation of phenological activity. One way to address this challenge is to integrate remotely sensed observations obtained at different spatial and temporal scales to provide information that contains both high temporal density and fine spatial resolution observations. In this article, we compare measures of vegetation phenology observed from a network of ground-based cameras with satellite-derived measures of greenness derived from a fused broad (MODIS) and fine spatial (Landsat) scale satellite data set. We derive and compare three key indicators of phenological activity including the start date of green-up, start date of senescence and length of growing season from both a ground-based camera network and 30 m spatial resolution synthetic Landsat scenes. Results indicate that although field-based estimates, generally, predicted an earlier start and end of the vegetation season than the fused satellite observations, highly significant relationships were found for the prediction of the start ($R^2 = 0.65$), end ($R^2 = 0.72$) and length ($R^2 = 0.70$) of the growing season across all sites. We conclude that some predictable bias exists however unlike visual field measures of the collected data represent both a spectral and a visual archive for later use.

*Corresponding author. Email: nicholas.coops@ubc.ca

Remote Sensing Letters
ISSN 2150-704X print/ISSN 2150-7058 online
http://www.tandf.co.uk/journals
DOI: 10.1080/01431161.2010.550330

1. Introduction

Information on the timing of reoccurring biological events such as leaf emergence, peak leaf area and senescence are important indicators of vegetation phenology. For instance, changes in the timing of plant phenology may signal important inter-annual climatic variations (Reed *et al.* 1994) and are therefore a crucial factor for the carbon balance of terrestrial ecosystems (Keeling *et al.* 1996, Kang *et al.* 2003, Badeck *et al.* 2004). The phenological cycle of vegetation is also a critical driver of food availability and animal habitat use for a wide range of species, such as the grizzly bear (*Ursus arctos* L.), whose foraging activities are known to be highly seasonal (Munro *et al.* 2006, Nielsen *et al*. 2010).

Traditionally, assessment of changes in phenology of food resources for fauna has relied on field measurements, often by volunteers and amateur naturalists, who record discrete events such as flowering, leaf emergence and other characteristics depending on observation goals and site location (Richardson *et al.* 2007). Although these observations are a valuable source of information, they are limited in spatial coverage and make use of a range of methodologies conducted by a large number of personnel with variable training and skill levels resulting in highly variable data consistency and quality.

As an alternative to traditional field-based measurements, a number of remote sensing techniques have been developed to observe vegetation cycles throughout the year. At the stand level, the increasing popularity and use of inexpensive visible spectrum digital cameras has offered a new source of information for the monitoring and measurement of phenological events at the local scale (Woebbecke *et al.* 1995, Graham *et al.* 2010, Ide and Oguma 2010). Repeat photography allows a very fine temporal sampling, often at daily or hourly intervals, for monitoring vegetation phenology. By mounting these systems on towers, other vertical objects or surface platforms, data can be acquired at an intermediate scale of observation, providing a link between field-based observation methods and satellite-derived estimates. At the satellite level, field-based assessments have been successfully linked to multispectral images of different spatial resolutions. For instance, estimates of vegetation phenology have been compared with the data acquired from the National Oceanic and Atmospheric Administration (NOAA) AVHRR (Advanced Very High Resolution Radiometer; Schwartz *et al.* 2002, Studer *et al.* 2007), and more recently the MODIS (MODerate-resolution Imaging Spectroradiometer) instrument onboard the Terra and Aqua platforms (Fisher and Mustard 2007, Soudani *et al.* 2008).

A fundamental challenge faced when using remote sensing techniques to monitor vegetation phenology is the trade-off required between the level of spatial detail and the revisit time provided by the sensor. For instance, although the data from the Landsat series of satellites have been successfully used to map vegetation at a 30 m spatial resolution, its 16-day temporal resolution is often not sufficient for timely observation of changes in vegetation and landscape characteristics throughout the year (Gao *et al.* 2006), particularly in areas with persistent cloud cover that result in longer intervals between clear imagery suitable for analysis. In contrast, satellites with higher revisit rates often do not provide a sufficient level of spatial detail that makes species-specific phenological events difficult to ascertain and extract (Botta *et al.* 2000).

One way to address this challenge is to integrate remotely sensed observations obtained at different spatial and temporal scales to provide information that contains both a high temporal density and fine spatial scale observations. At the stand

level, images obtained from transects of phenological cameras (Bater *et al.* 2011) can be directly linked to satellite observations to upscale fine-scale information on vegetation green-up and senescence to larger areas. At the satellite level, data fusion approaches using sensors with complementary spatial and temporal characteristics have become powerful tools to improve the temporal density of medium-scale sensors, such as Landsat. For instance, the Spatially and Temporally Adaptive Reflectance Fusion Model (STARFM) (Gao *et al.* 2006) allows synthetic, Landsat-like, observations with a 30 m spatial resolution with a revisit time of the MODIS sensor by combining observations from both. As a result, these observations can reflect seasonal changes in vegetation phenology at a spatial resolution sufficiently fine to provide detailed information on different vegetation zones and land-cover types (Hilker *et al.* 2009), at time intervals with relevance to vegetation phenology and animal habitat selection.

In this letter we compare measures of vegetation phenology observed from a network of ground-based camera with satellite-derived measures of vegetation condition derived from a fused broad (MODIS) and fine (Landsat) spatial scale satellite data set using the STARFM algorithm. We derive and compare three key indicators of phenological activity across an elevation gradient of sites: specifically, start date of green-up, start date of green-down and length of growing season from both a ground-based camera network and a time series of 14-day synthetic 30 m Landsat scenes.

2. Materials and methods

2.1 *Study area*

The study sites are located within the foothills of western Alberta, Canada, on the eastern slopes of the Rocky Mountains. To assess the capacity of the camera network to detect phenological variability across a range of site conditions, six sites were selected at three different elevation zones to reflect the coniferous and broadleaf-dominated vegetation types. One site was placed within a coniferous-dominated stand, and the other site located in a more mixed species site with between 20% and 40% deciduous species. Additionally, a seventh site was established in a high elevation coniferous stand. Details on the sites, their vegetation composition and location are summarized in table 1 (Bater *et al.* 2011).

2.2 *Digital camera network set-up*

In summary, seven standard commercially available digital camera systems manufactured by Harbortronics (Fort Collins, CO, USA) were installed (with the network described in detail in Bater *et al*. (2011)). The systems consist of a Pentax digital single lens reflex camera slaved to an intervalometer, which are sealed in a fibreglass case and powered by a solar panel and battery. Each digital single lens reflex were configured with either 6.1 or 10.2 million pixel image sensors with red green blue (RGB) images acquired at noon local time. Woebbecke *et al*. (1995) determined that the 2G-RBi which compared the green channel of the RGB image with the radiance in the red and blue regions, was particularly effective. 2G-RBi is calculated using the following equation:

$$2\mathrm{G} - \mathrm{RBi} = 2\mu_{\mathrm{G}} - (\mu_{\mathrm{R}} + \mu_{\mathrm{B}}), \tag{1}$$

Table 1. Summary of the camera sites, including forest cover type and coordinates.

Site name	Easting (m)[1]	Northing (m)[1]	Forest type	Forest composition and common names (basal area)	Elevation (m)[2]
Bryan spur	502,319	5,899,684	Mixed	Lodgepole pine (16 m^2/ha), trembling aspen (10 m^2/ha), and spruce species (2 $m^{2/}$ha)	1093
Bryan spur	501,950	5,898,930	Coniferous	Open black spruce forest (10 m^2/ha), bog	1092
Fickle Lake	519,136	5,916,668	Mixed	White spruce (22 m^2/ha), trembling aspen (18 m^2/ha), dead balsam poplar (4 m^2/ha), closed forest	970
Fickle Lake	518,537	5,916,058	Coniferous	Riparian white spruce forest (14 m^2/ha), bog	951
Cadomin	478,427	5,877,276	Mixed	Riparian, balsam poplar (6 m^2/ha) and white spruce (4 m^2/ha)	1484
Cadomin	480,660	5,879,755	Coniferous	Open black spruce forest (6 m^2/ha), occasional lodgepole pine, bog	1458
Prospect Creek	478,036	5,868,840	Coniferous	High elevation, lodgepole pine (20 m^2/ha)	1714

Notes: [1]Horizontal Datum: World Geodetic System 1984. Projection: Universal Transverse Mercator. Zone: 11 north.
[2]Ellipsoid: World Geodetic System 1984.

where μ_G, μ_R and μ_B are the camera-observed brightness values (raw DN) in the green, red and blue channels. Recently, this index has been more widely adopted using ground-based true colour digital imagery for vegetation monitoring. For example, Richardson *et al.* (2007) developed a phenological camera network using an RGB camera system and found good correlations between the 2G-RBi and vegetation gross primary production as measured from an eddy flux covariance tower. Once the index is calculated for all of the camera images, information on key dates, such as the start and end of the growing season, is estimated (Waring *et al.* 2006). One approach to extract these dates is used as the seasonal midpoint (or half-maximum approach), which was designed to predict the initial leaf expansion of broadleaf forests (White *et al.* 1999, Schwartz *et al.* 2002, Bater *et al.* 2011). This method first calculates the annual minimum and maximum value for each pixel and then a midpoint is calculated and added to the minimum. This calculated value has the advantage over other formulations as it is sensitive to site-specific variations in the range of values and may be more sensitive to local variation in canopy leaf area and chlorophyll concentrations (Waring *et al.* 2006).

2.3 *MODIS/Landsat STARFM data*

Landsat imagery with a 30 m spatial resolution over a 185 × 185 km scene extent is well suited to characterizing landscape-level forest structure and dynamics (Wulder *et al*. 2008). Although Landsat images have a useful spatial resolution for describing vegetation properties, the Landsat orbital repeat pass of 16 days, combined with the

impact of cloud cover on any given acquisition, makes it unsuitable for monitoring monthly or seasonal patterns. MODIS has a higher temporal resolution, enabling the characterization of a given location on a daily basis; however, the sensor has a spatial resolution of 250 m and above. Through fusing Landsat and MODIS imagery, we have the capacity to exploit the spatial detail of Landsat with the temporal regularity of MODIS acquisitions.

The STARFM predicts reflectance at up to daily time steps, depending on the availability of MODIS data. STARFM uses a spatially weighted difference between the Landsat and the MODIS scenes acquired at time-1 (T1), one or more of the Landsat scenes acquired at the same date(s) and one or more MODIS scenes of prediction day (T2), to predict pixel values, respectively (Gao *et al.* 2006). If more than one Landsat scene is provided, the 30 m resolution data are weighted according to the proximity of the T2 prediction scene. A moving window technique is used to minimize the effect of pixel outliers thereby predicting changes of the centre pixel using the spatially and spectrally weighted mean difference of pixels within the window area (Gao *et al.* 2006). Hilker *et al.* (2009) found that on a channel-by-channel basis, the surface reflectance values (stratified by broad land-cover types) of four actual Landsat images with the corresponding closest date of synthetic Landsat imagery were not statistically different between real (observed) and synthetic (predicted) reflectance. Similarly, a pixel-based analysis shows that predicted and observed reflectance values for the four Landsat dates were closely related ($R^2 = 0.76$, $p < 0.01$). A full description of the STARFM algorithm can be found in Gao *et al.* (2006) and Hilker *et al.* (2009), with the latter algorithm updated to aid in the characterization of change over time.

In this study we utilized the 8-day MODIS Nadir Bi-directional reflectance distribution function atmospherically corrected surface reference products (MOD43B4) from February to September 2009, resulting in a total of 32 MODIS scenes. Two Landsat scenes acquired on 27 August and 12 September 2009 were used as the high spatial resolution STARFM input. Synthetic Landsat scenes were generated to coincide with each of the MODIS 8-day composites. Once processed, the Normalized Difference Vegetation Index (NDVI), an index of vegetation condition that uses the near-infrared (NIR) and red bands from the Landsat imagery, and the 2G-RBi, described above from the phenological camera network, were calculated. Statistical analysis was undertaken by comparing the computed start and end of growing season, as well as the length of growing season, derived using the seasonal midpoint (or half-maximum approach).

3. Results

Throughout the observation period, an excess of 6700 images were acquired at the 7 sites by the phenological camera network. NDVI from the synthetic Landsat imagery (STARFM) and 2G-RBi camera temporal spectral indices are shown for the example of the Bryan spur-mixed site in figure 1. Figure 1(*a*) shows the NDVI time series derived from STARFM and figure 1(*b*) shows the camera observations for the same site. In both cases, a 4th order polynomial (based on the work of Ahrends *et al*. 2008) has been fitted to quantify the seasonal change in NDVI and 2G-RBi, respectively. The grey lines illustrate the estimated start and end of the vegetation period derived from the half min/max threshold of both curves. Although the phenological cameras had no NIR channel available to derive vegetation greenness from ground-based NDVI time series, the 2G-RBi served as a useful surrogate to measure the vegetation greenness.

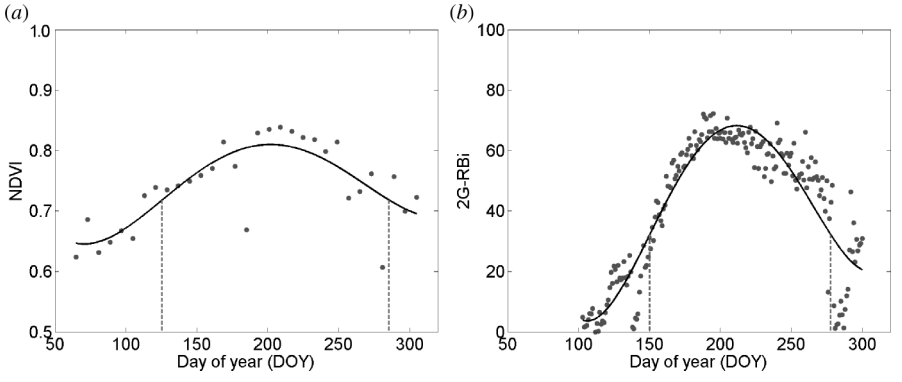

Figure 1. Example of temporal sequence of (*a*) NDVI STARFM predictions and (*b*) 2G-RBi camera values for a mixed deciduous and a coniferous site in the study area with the fitted 4th order polynomial shown in grey.

Although it would have also been possible to derive a 2G-RBi from STARFM data, measurement of vegetation greenness from only the visible channels is less desirable from spaceborne observations, as (1) the blue channel is often prone to atmospheric effects and noise that are difficult to correct and (2) the signal-to-noise ratio of NDVI is usually much higher than for an index derived from visible bands, due to the stronger reflectance in the NIR channel.

The implementation of the half-maximum parameter approach produced a range of start and end of growing season dates across the 7 sites that ranged from day 106 as observed by the camera network to day 137 as observed from the STARFM data. Similarly, the growing season length as estimated using the half-maximum method ranged from 93–107 days for the field observations to 104–120 days using the STARFM data. Figure 2 shows a comparison between start, end and length of vegetation season observed by the phenological cameras and STARFM data. The field-based estimates, generally, predicted an earlier start and end of the vegetation season due to the different absolute values obtained from NDVI and 2G-RBi. Significant relationships were found for the prediction of the start ($R^2 = 0.65$), end ($R^2 = 0.72$) and length ($R^2 = 0.70$) of the growing season across all seven sites.

Figure 3 shows an estimate for (*a*) start and (*b*) length of the growing season for Landsat path/row 44/23, in which all the field sites were located. Start and length of vegetation season have been predicted using the half-maximum method of the STARFM time series. The growing season started earliest in the low elevation, flat regions of the boreal forest landscape shown in the north-west region of this map, whereas the mountainous areas had the shortest growing season, with late green-up dates and moderately early leaf-down estimates. The areas with no data correspond to lakes or alpine exposed rock, for which no seasonal differences were observed. As would be anticipated, the start of the growing season was, generally, later, and the length of growing season shorter for high elevation sites compared with those at lower elevations.

4. Discussion and conclusion

This study expands on the previous work in two key ways. First, we continue to develop, with others, the applicability of digital camera networks to the study of phenological indicators, with specific reference in our research towards the development

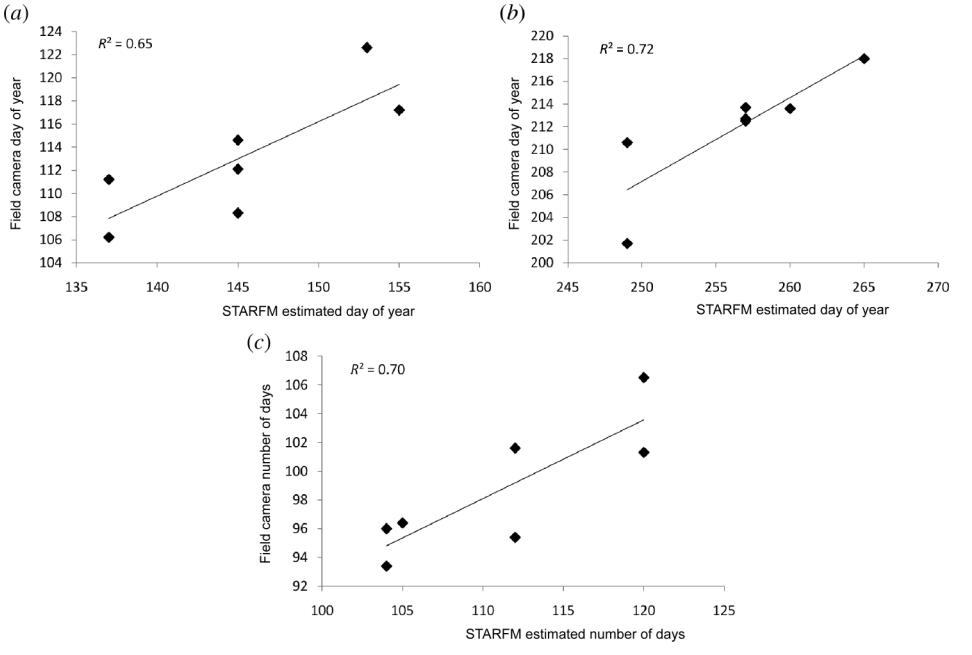

Figure 2. Relationship between digital camera 2G-RBi and STARFM NDVI half-maximum values for (*a*) the start of growing season ($R^2 = 0.65$, $p < 0.001$, standard error of estimate in days = 4.5), (*b*) the end of growing season ($R^2 = 0.72$, $p < 0.001$, standard error of estimate in days = 3.3) and (*c*) the length of growing season ($R^2 = 0.70$, $p < 0.001$, standard error of estimate in days = 4.2).

of spatially explicit models shifting food availability and habitat resources for fauna at spatial and temporal scales relevant to animal activities (e.g. Nielsen *et al.* 2010). The accurate discrimination of vegetation from ground-based camera networks is an active research area in a number of fields. For example, the application of automated remote sensing and machine vision to the automatic assessment of crops and weeds in precision crop management is a rapidly increasing field, where the imagery is used to discriminate between the two and then apply appropriate levels of fertilizer and weed control (Meyer and Neto 2008, Slaughter *et al.* 2008).

Our work continues the research of Richardson *et al.* (2007) and Ahrends *et al.* (2008) by demonstrating the link between ground-based cameras and satellite observations at the Landsat and MODIS scale. In Ahl *et al.* (2006), several standard MODIS products with different spatial and temporal resolutions were used. Overall products that had the least amount of spatial and temporal smoothing (or processing steps) produced the best agreement between predictions and field observations. For example, the 250 m daily NDVI estimates were more consistent and precise compared with field observations than the 16-day composite MODIS vegetation index products. This finding is consistent with Turner *et al.* (2003) who suggested that because many MODIS 8-day composites are derived from maximum values, they should predict onset of green-up earlier than the field. This response, however, could be counteracted by the influence of topographic variation within MODIS cells causing a mixed temporal response.

Our results indicate that some bias exists between the timing of the half-maximum onset and end and length of growing season derived from ground-based cameras, as well as synthetic Landsat STARFM predictions. Although the camera data provide

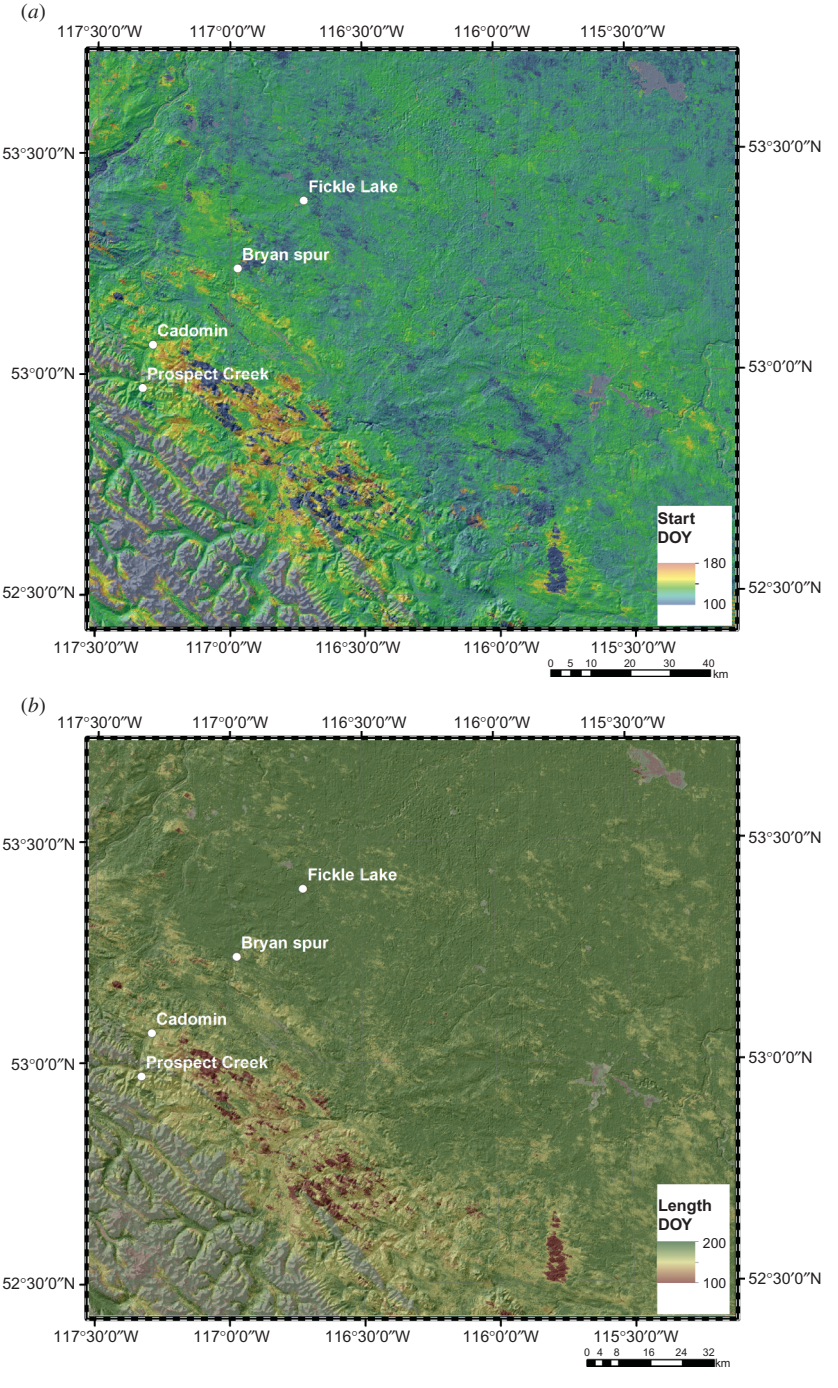

Figure 3. STARFM-based estimates of start and length of the growing season using the half min/max threshold. The displayed area corresponds to Landsat path/row 44/23 and the location of the field sites is provided for orientation.

a daily indication of greenness, it is influenced by hourly, daily and seasonal changes in illumination. The STARFM observations, on the contrary, are based on the 8-day MODIS composites scaled by Landsat observations, but both are at a larger spatial resolution than the field of view of the camera. Nonetheless, the cameras effectively captured a range of phenological conditions for multiple species found at sites along the transect, and the data they collect represent both a spectral and visual record for later use. The standard error of the relationship between the two sets of observations is between 3 and 4 days indicating that once the delay in green-up as observed by the satellite sensors is accounted for, the overall relationship with ground-based observations is very good. As part of our ongoing work, these models of phenological development will be expanded to cover key plant species that form critical components of grizzly bear (*Ursus arctos* L.) diets, and from these relationships, we anticipate that we will then be able to spatially predict the green-up, budding and fruiting of key species across the landscape.

Acknowledgements

Sam Coggins (University of British Columbia) and David Laskin (University of Calgary) were members of the deployment team. Andrew Richardson (Harvard University) and Scott Ollinger (University of New Hampshire) provided initial advice and enthusiasm for the network plans. Funding for this research was generously provided by the Grizzly Bear Program of the Foothills Research Institute located in Hinton, AB, Canada, with additional information available at http://www.foothillsresearchinstitute.ca/.

References

Ahl, D.E., Gower, S.T., Burrows, S.N., Shabanov, N.V., Myneni, R.B. and Knyazikhin, Y., 2006, Monitoring spring canopy phenology of a deciduous broadleaf forest using MODIS. *Remote Sensing of Environment*, **104**, pp. 88–95.

Ahrends, H.E., Brügger, R., Stöcklii, R., Schenk, J., Michna, P., Jeanneret, F., Wanner, H. and Eugster, W., 2008, Quantitative phenological observations of a mixed beech forest in northern Switzerland with digital photography. *Journal of Geophysical Research*, **113**, p. G04004.

Badeck, F., Bondeau, A., Bottcher, K., Doctor, D., Lucht, W., Schaber, J. and Sitch, S., 2004, Responses of spring phenology to climate change. *New Phytologist*, **162**, pp. 295–30.

Bater, C.W., Coops, N.C., Wulder, M.A., Nielsen, S.E., Mcdermid, G. and Stenhouse, G.B., 2011, Design and installation of a camera network across an elevation gradient for habitat assessment. *Instrumentation Science & Technology*, **39**, pp. 231–247.

Botta, A., Viovy, N., Ciais, P., Friedlingstein, P. and Monfray, P., 2000, A global prognostic scheme of leaf onset using satellite data. *Global Change Biology*, **6**, pp. 709–725.

Fisher, J.I. and Mustard, J.F., 2007, Cross-scalar satellite phenology from ground, Landsat, and MODIS data. *Remote Sensing of Environment*, **109**, pp. 261–273.

Gao, F., Masek, J., Schwaller, M. and Hall, F., 2006, On the blending of the Landsat and MODIS surface reflectance: predicting daily Landsat surface reflectance. *IEEE Transactions on Geoscience and Remote Sensing*, **44**, pp. 2207–2218.

Graham, E.A., Riordan, E.C., Yuen, E.M., Estrin, D. and Rundel, P.W., 2010, Public Internet-connected cameras used as a cross-continental ground-based plant phenology monitoring system. *Global Change Biology*, **16**, pp. 3014–3023.

Hilker, T., Wulder, M.A., Coops, N.C., Seitz, N., White, J.C., Gao, F., Masek, J.G. and Stenhouse, G., 2009, Generation of dense time series synthetic Landsat data through

data blending with MODIS using a spatial and temporal adaptive reflectance fusion model. *Remote Sensing of Environment*, **113**, pp. 1988–1999.

Ide, R. and Oguma, H., 2010, Use of digital cameras for phenological observations. *Ecological Informatics*, **5**, pp. 339–347.

Kang, S., Running, S.W., Lim, J.-H., Zhao, M., Park, C. and Loehman, R., 2003, A regional phenology model for detecting onset of greenness in temperate mixed forests, Korea: an application of MODIS leaf area index. *Remote Sensing of Environment*, **86**, pp. 232–242.

Keeling, C.D., Chin, J.F. and Whorf, T.P., 1996, Increased activity of northern vegetation inferred from atmospheric CO_2 measurements. *Nature*, **382**, pp. 146–149.

Meyer, G.E. and Neto, J.C., 2008, Verification of color vegetation indices for automated crop imaging applications. *Computers and Electronics in Agriculture*, **63**, pp. 282–293.

Munro, R.H., Nielsen, S.E., Price, M.H., Stenhouse, G.B. and Boyce, M.S., 2006, Seasonal and diel patterns of grizzly bear diet and activity in west-central Alberta. *Journal of Mammology*, **87**, pp. 1112–1121.

Nielsen, S.E., McDermid, G., Stenhouse, G.B. and Boyce, S.E., 2010, Dynamic wildlife habitat models: seasonal foods and mortality risk predict occupancy-abundance and habitat selection in grizzly bears. *Biological Conservation*, **143**, pp. 1623–1634.

Reed, B.C., Brown, J.F., Vanderzee, D., Loveland, T.R., Merchant, J.W. and Ohlen, D.O., 1994, Measuring phenological variability from satellite imagery. *Journal of Vegetation Science*, **5**, pp. 703–714.

Richardson, A., Jenkins, J., Braswell, B., Hollinger, D., Ollinger, S. and Smith, M., 2007, Use of digital webcam images to track spring green-up in a deciduous broadleaf forest. *Oecologia*, **152**, pp. 323–334.

Schwartz, M.D., Reed, B.C. and White, M.A., 2002, Assessing satellite-derived start-of-season measures in the conterminous USA. *International Journal of Climatology*, **22**, pp. 1793–1805.

Slaughter, D.C., Giles, D.K. and Downey, D., 2008, Autonomous robotic week control systems: a review. *Computers and Electronics in Agriculture*, **61**, pp. 63–78.

Soudani, K., le Maire, G., Dufrêne, E., François, C., Delpierre, N., Ulrich, E. and Cecchini, S., 2008, Evaluation of the onset of green-up in temperate deciduous broadleaf forests derived from Moderate Resolution Imaging Spectroradiometer (MODIS) data. *Remote Sensing of Environment*, **112**, pp. 2643–2655.

Studer, S., Stöckli, R., Appenzeller, C. and Vidale, P.L., 2007, A comparative study of satellite and ground-based phenology. *International Journal of Biometeorology*, **51**, pp. 405–414.

Turner, D.P., Ritts, W.D., Cohen, W.B., Gower, S.T., Zhao, M., Running, S.W., Wofsy, S.C., Urbanski, S., Dunn, A.L. and Munger, J.W., 2003, Scaling Gross Primary Production (GPP) over boreal and deciduous forest landscapes in support of MODIS GPP product validation. *Remote Sensing of Environment*, **88**, pp. 256–270.

Waring, R.H., Coops, N.C., Fan, W. and Nightingale, J.M., 2006, MODIS enhanced vegetation index predicts tree species richness across forested ecoregions in the contiguous U.S.A. *Remote Sensing of Environment*, **103**, pp. 218–226.

White, M.A., Running, S.W. and Thornton, P.E., 1999, The impact of growing-season length variability on carbon assimilation and evapotranspiration over 88 years in the eastern U.S. deciduous forest. *International Journal of Biometeorology*, **42**, pp. 139–145.

Woebbecke, D.M., Meyer, G.E., Von Bargen, K. and Mortensen, D.A., 1995, Color indices for weed identification under various soil, residue, and lighting conditions. *Transactions of the American Society of Agricultural Engineers*, **38**, pp. 259–269.

Wulder, M.A., White, J.C., Goward, S.N., Masek, J.G., Irons, J.R., Herold, M., Cohen, W.B., Loveland, T.R. and Woodcock, C.E., 2008, Landsat continuity: issues and opportunities for land cover monitoring. *Remote Sensing of Environment*, **112**, pp. 955–969.